NeuroImage 168 (2018) 452–458

Contents lists available at ScienceDirect

NeuroImage

journal homepage: www.elsevier.com/locate/neuroimage

Clinical vascular imaging in the brain at 7 T☆

Laurens JL De Cocker[a,b,*], Arjen Lindenholz[a], Jaco JM Zwanenburg[a], Anja G van der Kolk[a], Maarten Zwartbol[a], Peter R Luijten[a], Jeroen Hendrikse[a]

[a] Department of Radiology, University Medical Center Utrecht, The Netherlands
[b] Department of Radiology, Kliniek Sint-Jan, Brussels, Belgium

A B S T R A C T

Stroke and related cerebrovascular diseases are a major cause of mortality and disability. Even at standard-field-strengths (1.5 T), MRI is by far the most sensitive imaging technique to detect acute brain infarctions and to characterize incidental cerebrovascular lesions, such as white matter hyperintensities, lacunes and microbleeds. Arterial time-of-flight (TOF) MR angiography (MRA) can depict luminal narrowing or occlusion of the major brain feeding arteries, and this without the need for contrast administration. Compared to 1.5 T MRA, the use of high-field strength (3 T) and even more so ultra-high-field strengths (7 T), enables the visualization of the lumen of much smaller intracranial vessels, while adding a contrast agent to TOF MRA at 7 T may enable the visualization of even more distal arteries in addition to veins and venules. Moreover, with 3 T and 7 T, the arterial vessel walls beyond the circle of Willis become visible with high-resolution vessel wall imaging. In addition, with 7 T MRI, the brain parenchyma can now be visualized on a submillimeter scale. As a result, high-resolution imaging studies of the brain and its blood supply at 7 T have generated new concepts of different cerebrovascular diseases. In the current article, we will discuss emerging clinical applications and future directions of vascular imaging in the brain at 7 T MRI.

1. Introduction

Vascular disorders of the brain, including stroke, are a major cause of death in addition to physical and cognitive disability. During the past decades, imaging has become an indispensable tool in the work-up, treatment planning and follow-up of ischemic and hemorrhagic stroke, as well as in the identification of cerebrovascular anomalies predisposing to stroke. In addition, imaging may record the burden of incidental cerebrovascular lesions that may lead to pathologic brain aging. Compared to CT and other imaging modalities, brain magnetic resonance imaging (MRI) is by far the best technique to assess the total extent of cerebrovascular diseases in individual patients, as it allows for the accurate visualization of acute and chronic manifestations of large- and small-vessel disease in both the supra- and infratentorial regions. Although routine clinical practice is currently still limited to standard (1.5 T) and high-field (3 T) MRI, cerebrovascular disease evaluation at ultra-high-field (7 T) MRI may benefit from a high signal to noise ratio (SNR) which can be transferred into high spatial resolution, as well as a high contrast to noise ratio (CNR). By enabling the evaluation of the brain parenchyma on a submillimeter scale, very small cerebrovascular lesions, such as cortical microinfarcts, have come within the detection limit of 7 T and to a lesser degree 3 T MRI (van Dalen et al., 2015). Also, compared to 1.5 T arterial MR angiography (MRA), the use of high-field (3 T) and even more so ultra-high field MRI (7 T), has enabled the visualization of the lumen of much more peripheral intracranial vessels, and of the intracranial vessel walls of the circle of Willis (CoW) and beyond (Harteveld et al., 2015; Dieleman et al., 2014a). Finally, MR perfusion weighted imaging (PWI) may benefit from 7 T, for instance by the increased susceptibility effects and the lower amount of contrast agent required for dynamic susceptibility contrast (DSC) perfusion at 7 T. Thus, the advent of 7 T has during the past decade resulted in a wave of research exploring new developments in cerebrovascular imaging, which are now increasingly finding their way into clinical practice. In the current article, we will review the emerging clinical applications and future directions of vascular imaging in the brain at 7 T.

2. Clinical applications

A clinically feasible stroke imaging protocol at 7 T has already been proposed and investigated for subacute and chronic stroke patients (Madai et al., 2012). This imaging protocol includes T1-weighted 3D

☆ Invited Review Article for 'Neuroimaging with Ultra-High Field MRI: Present and Future'.

* Correspondence to: Department of Radiology, Kliniek Sint-Jan, Kruidtuinlaan 32, 1000 Brussels, Belgium.
E-mail address: laurens_de_cocker@hotmail.com (L.J. De Cocker).

http://dx.doi.org/10.1016/j.neuroimage.2016.11.044
Accepted 16 November 2016
Available online 18 November 2016

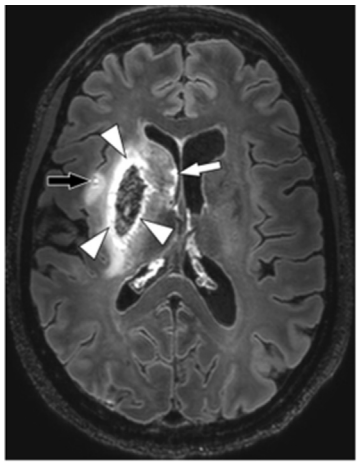

Fig. 1. Ultra-high resolution imaging of ischemic stroke. Axial 7 T contrast-enhanced 3D-FLAIR image of 50-year-old female with a recent right-sided ischemic stroke with hemorrhagic transformation, repetition time 8000ms, echo time 300ms, inversion time 2200 ms, acquired voxel size 0.8×0.8×0.8 mm^3, reconstructed voxel size 0.5×0.5×0.5 mm^3, field-of-view 250x250×190 mm^3, scan duration 10:48 min. A hyperintense border is seen to surround the lentiform nucleus (putamen and globus pallidus, arrowheads), which appears hypointense due to blood components. A smaller infarct is also seen in the insular region (black arrow), and multiple hyperintense dots are also seen along the ventricular border of the head of the caudate nucleus (white arrow), all of which are compatible with satellite infarctions.

Magnetization-Prepared Rapid-Acquired Gradient-Echo (3D-MPRAGE), T2-weighted 2D Fluid Attenuated Inversion Recovery (2D-FLAIR), T2-weighted 2D Turbo Spin Echo (2D-T2-TSE), T2*-weighted 2D Fast Low Angle Shot Gradient Echo (2D-HemoFLASH) and 3D arterial Time-of-Flight (TOF) MRA. However, the imaging protocol excludes diffusion weighted imaging (DWI), the most sensitive imaging technique to detect acute infarctions (Madai et al., 2012). With improvements being made to DWI at 7 T, it may be expected that clinical stroke protocols at 7 T imaging will be extended to include acute stroke patients as well.

2.1. Ischemic stroke

About 80% of strokes are ischemic and about 20% hemorrhagic in origin. Hemorrhagic transformation is a not infrequent complication of ischemic stroke and Fig. 1 shows an axial 7 T FLAIR image of a patient with ischemic stroke undergoing hemorrhagic transformation in the territory of the right middle cerebral artery. The figure displays the high degree of detail discernible with 7 T in stroke patients (Madai et al., 2012). Most ischemic strokes have an extracranial origin and result either from cardio-embolism or artery-to-artery embolism from the carotid or vertebrobasilar arteries. Screening for cardiac arrhythmia and evaluation of the neck vessels may point towards the correct stroke origin in most of these patients. In case of artery-to-artery embolism from the neck, luminal imaging may reveal arterial stenosis, most frequently at the level of the carotid bifurcation.

In a considerable proportion of patients, however, the origin of stroke may be related to intracranial arterial lesions, evaluation of which may especially benefit from high-resolution MR imaging. Not unlike arterial lesions in the neck, intracranial arterial lesions include atherosclerotic plaques, and, more rarely, dissection or vasculitis.

2.1.1. Intracranial atherosclerosis

Arterial TOF MRA is routinely performed in stroke patients to detect intracranial arterial stenosis, and is usually preferred above angiographic techniques (CTA and DSA) because of its non-invasiveness, the lack of ionizing radiation, and no need to administer a contrast medium (Fig. 2). Also, it can be acquired in the same imaging session as DWI, the most sensitive technique to detect acute infarction.

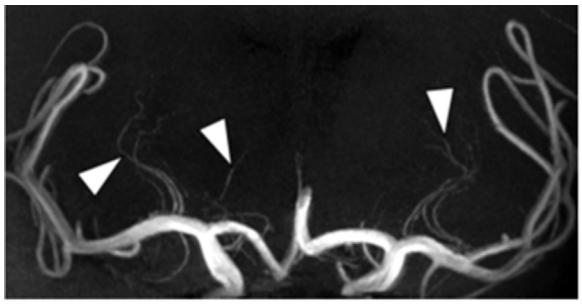

Fig. 2. MR Angiography of the intracranial perforating arteries. MR Angiography of the intracranial perforating arteries. Coronal Maximum Intensity Projection (MIP) of a 7 T Time-of-Flight (TOF) MRA, repetition time 16ms, echo time 3.3 ms, acquired voxel size 0.25×0.3×0.4 mm^3, reconstructed voxel size 0.2×0.2×0.2 mm^3, field-of-view 200x190×50 mm^3, scan duration 9:54 min, performed in a 51-year-old male. Perforating lenticulostriate arteries (arrowheads) branching off from the middle cerebral arteries are clearly seen in both cerebral hemispheres.

Compared to 1.5 T and 3 T, arterial TOF MRA at 7 T allows the visualization of much smaller intracranial arteries, such as the lenticulostriate arteries (Fig. 2), while adding a contrast agent may enable the visualization of even more distal arteries in addition to veins and venules (Harteveld et al., 2015; Madai et al., 2012; Kang et al., 2010). The presence of intracranial arterial narrowing alone, however, does not necessarily correspond to a stroke origin; arterial stenosis may already have been present a long time before the onset of stroke, and may be compensated by adequate primary (circle of Willis) or secondary (leptomeningeal) collaterals (Liebeskind et al., 2011; Hartkamp et al., 2016). In addition, atherosclerotic plaques may be present without luminal narrowing due to arterial remodeling (Qiao et al., 2016). Because of the shortcomings of lumenography, there is a need for intracranial vessel wall imaging to link cerebral infarction with intracranial arterial lesions, such as symptomatic plaques, dissection or vasculitis. Because of the small caliber of intracranial arteries, a high SNR which can be transferred into high spatial resolution, as well as a high CNR are required for visualization of the pathologic vessel wall, and even more so for the healthy vessel wall (Fig. 3) (Dieleman et al. 2014a). Since spatial resolution increases with field strength, (ultra-) high field imaging techniques are required to visualize wall thickening of arteries of the circle of Willis and beyond (Dieleman et al., 2014a). Also, for optimal vessel wall visualization, signal suppression of the

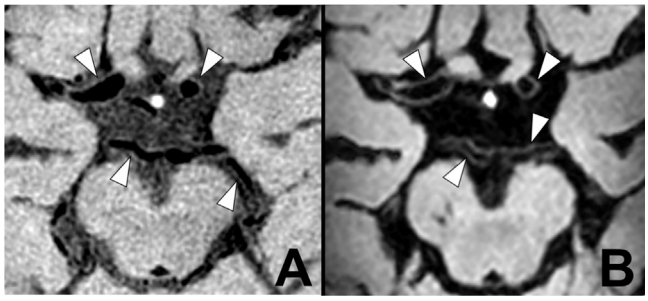

Fig. 3. Intracranial vessel wall imaging at 3 T and 7 T. Intracranial vessel wall imaging at 3 T and 7 T. Intracranial vessel wall imaging of a 71 year-old-male with a recent left sided ischemic infarction in the anterior circulation (not shown) resulting from symptomatic carotid artery disease. (A) A transverse 3 T contrast-enhanced T1 Volume Isotropically Reconstructed Turbo Spin Echo Acquisition (VIRTA), repetition time 1500 ms, echo time 36 ms, acquired voxel size 0.6×0.6×1.0 mm^3, reconstructed voxel size 0.5×0.5×0.5 mm^3, field-of-view 200x167×45 mm^3, scan duration 6:42 min (Dieleman et al., 2016b). Most of the arterial vessel walls of the circle of Willis are visible and appear to be normal (arrowheads). Blood is more suppressed than cerebrospinal fluid. (B) A transverse 7 T post-contrast T1 Magnetization Preparation Inversion Recovery (MPIR) TSE acquisition, repetition time 3952ms, echo time 37ms, inversion time 1375, acquired voxel size 0.8×0.8×0.8mm^3, reconstructed voxel size 0.5×0.5×0.5 mm^3, field-of-view 250x250×190 mm^3, scan time 10:40 min (van der Kolk et al., 2011, 2013) The arterial vessel walls (arrowheads) are better seen due to an improved contrast with blood and cerebrospinal fluid, which is almost completely suppressed.

arterial lumen (black blood imaging techniques including double inversion recovery and techniques based on motion-sensitizing prepulses) is required for delineation of the inner vessel wall (Figs. 3A and B), while cerebrospinal fluid (CSF) suppression facilitates the demarcation of the outer vessel wall (Fig. 3B), especially for the more peripheral vessels surrounded by subarachnoid (CSF) spaces in case of cerebral atrophy (Dieleman et al., 2014a). However, acquisition of 3D isotropic sequences with high resolution and sufficient brain coverage result in relatively long scan times (Fig. 3) (Dieleman et al., 2014a; van der Kolk et al., 2011). Compared to 3 T imaging, the increased signal-to-noise ratio (SNR) of 7 T leads to an overall better vessel wall visibility, visualizes more atherosclerotic plaques, and thus offers the highest potential to identify the total burden of intracranial atherosclerosis (Harteveld et al., 2016; Zhu et al., 2016). Recently, several studies investigating the relationship between intracranial vessel wall changes on 3 T and 7 T and brain infarction have been published (Dieleman et al., 2014b; 2016a, 2016b). Although most studies have so far only been performed in a limited number of patients, the following preliminary conclusions may be drawn. Eccentric atherosclerotic lesions are most frequently detected and seem to be associated with a focal (short-segment) thickening pattern, while concentric plaques usually show a more diffuse (long-segment) thickening (Dieleman et al., 2016b). Although contrast-enhancement of intracranial atherosclerotic plaques is frequently observed and has been linked to the vessels supplying the area of ischemic injury, it may as well appear in asymptomatic lesions (Harteveld et al., 2016; Dieleman et al., 2016b; Aoki et al., 1995; Swartz et al., 2009). Since atherosclerotic lesions of the intracranial vasculature cannot be correlated with histopathology in living patients (unlike the carotid plaques, which may be surgically removed by endarterectomy), only post-mortem quantitative MRI-pathologic correlation studies have been performed to compare plaque contents with plaque signal intensities on 3 T and 7 T on CoW specimens (Harteveld et al., 2016; Jiang et al., 2016; Majidi et al., 2013; van der Kolk et al., 2015). These have shown the promising result that different tissue components of advanced intracranial plaques have distinguishable relaxation times on ultra-high-resolution quantitative MR imaging. T2 and T2* relaxation times at 3 T, and T1 relaxation times at 7 T, have shown the most differences among individual tissue components of intracranial plaques, including lipid, fibrous tissue, fibrous cap, calcifications, and the healthy vessel wall (Harteveld et al., 2016; Jiang et al., 2016). Hence, the most promising method for distinguishing intracranial plaque components at 7 T is T1-weighted imaging.

Intracranial dissection may be hard to diagnose due to the small caliber of the involved arteries, and thus its diagnosis may highly benefit from the spontaneous bright signal on T1 high-resolution vessel wall images, as has already been investigated at 3 T (Swartz et al., 2009; Arai et al., 2016). In addition, dissection often shows wall enhancement, and may present a visible flap and dual lumen (Swartz et al., 2009; Arai et al., 2016).

2.1.2. Vasculitis, reversible vasoconstriction syndrome and moyamoya

Central nervous system (CNS) vasculitis and reversible vasoconstriction syndrome (RCVS) often show clinical and lumenographic overlap, and at times only high-resolution vessel wall imaging with MRI may show distinguishing features between these two entities (Mandell et al., 2012; Obusez et al., 2014). CNS vasculitis is characterized by short segments of vessel wall thickening, which is concentric more often than eccentric, and is associated with vessel wall enhancement, which may resolve after healing (Swartz et al., 2009; Mandell et al., 2012; Obusez et al., 2014; Küker et al., 2008). Compared to CNS vasculitis, RCVS shows longer segments of reversible wall thickening, continuous throughout the entire wall of the diseased vessel, with no or only mild enhancement (Obusez et al., 2014). Furthermore, high-resolution intracranial vessel wall imaging at 3 T has been reported to be beneficial in differentiating moyamoya disease, atherosclerotic-moyamoya syndrome, and vasculitic-moyamoya syndrome (Mossa-Basha et al., 2016). Although vessel wall imaging studies at 7 T for moyamoya are still lacking, MPRAGE has already been found superior to TOF MRA at 7 T due to shorter scanning times and better brain coverage (Dengler et al., 2016).

2.2. Incidental or silent infarction and the aging brain

Apart from brain infarction presenting with stroke (Fig. 1), many (small) brain infarctions present with only few or non-specific clinical symptoms, or may even be clinically silent (Saini et al., 2012; Fanning et al., 2014; De Cocker et al., 2016). Still, these infarcts may present later on as an incidental finding on neuroimaging studies. They are associated with cognitive decline and worse physical functioning, and an increased risk of future stroke (Vermeer et al., 2003; Bernick et al., 2001; De Cocker et al., 2015). Traditionally, incidental cerebral infarctions include large and small cortical infarcts as well as subcortical infarcts, of which the latter includes lacunar infarcts (Riba-Llena et al., 2015; Longstreth et al., 1998; Del Bene et al., 2013; Wardlaw et al., 2013a).

2.2.1. Lacunar infarcts, perivascular spaces and white matter hyperintensities

Due to the superior evaluation of small-caliber arteries in the brain on 7 T arterial TOF MRA (Fig. 2), it has been found that the number of lenticulostriate arteries supplying the basal ganglia is reduced in patients with lacunes (of presumed vascular origin) compared to age-matched controls. This finding has later been translated to 1.5 T with flow-sensitive black blood MRA, suggesting that occlusion of lenticulostriate arteries underlies lacunar infarction of the basal ganglia (Kang et al., 2010; Wardlaw et al., 2013a; Okuchi et al., 2013). At times, lacunes may be difficult to distinguish from enlarged perivascular spaces (PVS), although the latter do not have a T2-hyperintense rim around the fluid-filled space on T2-weighted or FLAIR imaging, unless they traverse an area of white matter hyperintensity (Wardlaw et al., 2013a). At high resolution, a central vessel can occasionally be seen in the center of a perivascular space, which may differentiate the spaces from lacunes. (Wardlaw et al., 2013a; Zong et al., 2016). Also, optimized MRI parameters and segmentation methods have been developed for PVS at 7 T, which have shown that PVS are much more abundant than previously reported in young patients (Zong et al., 2016; Park et al., 2016). Despite the term lacunar infarction, it has been shown that only a small proportion of lacunar infarcts progress to lacunes (Potter et al., 2010; Moreau et al., 2012), and non-cavitating lacunar infarcts often continue to resemble white matter lesions instead (Wardlaw et al., 2013a; Potter et al., 2010). Also, in non-vascular disease such as multiple sclerosis (MS), characterization of white matter lesions with high resolution MR imaging has shown diagnostic benefits. With the increased SNR of 7 T MRI, the typical localization of MS plaques around small venules can be demonstrated (Ge et al., 2008; Tallantyre et al., 2008; Gizewski et al., 2015).

2.2.2. Cortical microinfarcts

Another major clinical advancement of 7 T MRI is its ability to detect cortical microinfarcts (CMIs) (Fig. 4). Historically being a strictly pathologic diagnosis recorded during autopsy in elderly people, high resolution MRI has made it possible to visualize some of these lesions in vivo at 7 T (Fig. 4) (Zwanenburg et al., 2012; van Veluw et al., 2012; van Veluw et al., 2015; Fracasso et al., 2016) and to a lesser degree at 3 T (van Dalen et al., 2015; van Veluw et al., 2015). Nevertheless, the majority of microinfarcts currently remain under the detection limits of clinical in vivo MRI (van Veluw et al., 2016). On post-mortem 7 T MRI studies, three types of CMIs have been distinguished based on the involvement of all three cortical layers (type 1), two cortical layers (type 2), or one (superficial, middle or deep) cortical

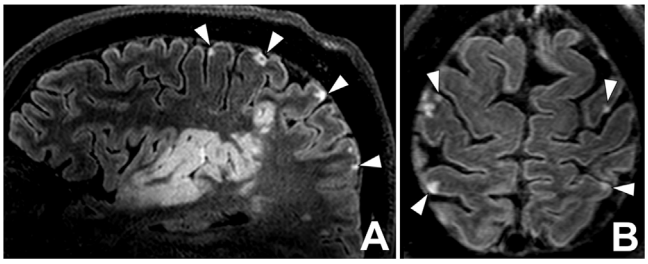

Fig. 4. Cortical microinfarcts**.** 7 T contrast-enhanced 3D-FLAIR imaging of a 68- year-old man with a large right-sided temporoparietal ischemic infarction (A), repetition time 8000ms, echo time 300ms, inversion time 2200 ms, acquired voxel size 0.8×0.8×0.8 mm^3, reconstructed voxel size 0.5×0.5×0.5 mm^3, field-of-view 250x250×190 mm^3, scan duration 10:48 min. (A) Sagittal and (B) axial reconstruction shows multiple tiny cortical hyperintensities, compatible with cortical microinfarcts. Most cortical microinfarcts seen involve all cortical layers, compatible with type I microinfarcts according to De Reuck et al., (2014).

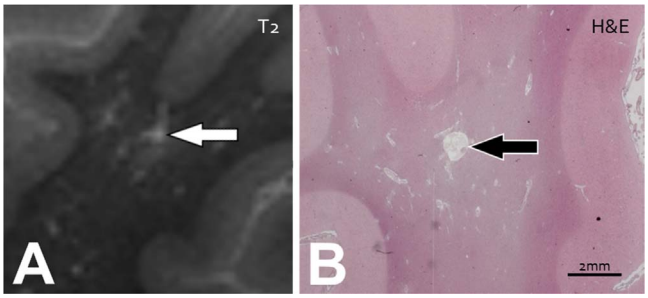

Fig. 5. Perivascular Spaces and Lacunar Infarcts. An example of a juxtacortical, enlarged perivascular space (PVS) mimicking a cerebral microinfarct (CMI), in a post-mortem brain of a 68-year-old female with Alzheimer's Disease pathology (BB VI) and severe cerebral amyloid angiopathy, identified on (A) T2-weighted ex vivo MR-imaging (repetition time 3500 ms, echo time 164 ms, acquired voxel size 0.4×0.4×0.4 mm^3, no SENSE acceleration, scan duration 112 min) and with (B) histopathological correlation, Hematoxylin & Eosin (H & E) staining. (A) The small hyperintense enlarged PVS is located in juxtaposition to the cortex (white arrow). (B) No evidence of neuronal death or gliosis is seen on H & E (black arrow). (images courtesy of S.J. van Veluw).

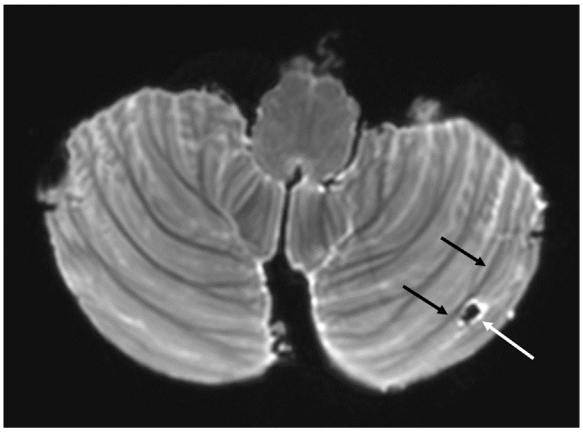

Fig. 6. Cerebellar cortical infarct cavity on 7 T post-mortem MRI**.** Cerebellar cortical infarct cavity (white arrow) in the left cerebellar hemisphere on T2-weighted 7 T post-mortem MRI; 3D TSE; TR 3000 ms; TE 207 ms; reduced focusing angle of 40°; acquired voxel size 0.70 × 0.70 × 0.70 mm^3; matrix size 284×169; FOV 200 × 119 x 120 mm^3; SENSE: 2×2; scan duration 8:39 min. The cavity and the surroundings of the cerebellum are black due to Fomblin, a proton-free fluid without MR signal. Notice the sharp demarcation of the cavity and surrounding hyperintense gliosis (white arrow) from the intact subjacent white matter (black arrows), which proved to be characteristic imaging features of cerebellar cortical infarct cavities and enabled the translation to clinical 1.5 T MRI scans (De Cocker et al., 2014; 2015).

layer only (type 3). (De Reuck et al., 2014). CMIs should be distinguished from enlarged or atypically shaped perivascular spaces, which can be CMI mimics but which are located juxtacortically (Fig. 5) (van Veluw et al., 2015). CMIs are associated with atherosclerosis, and are believed to be of microembolic origin (Zheng et al., 2013; Raman et al., 2014; Rotte et al., 2014). Also, CMIs are a new marker of vascular dementia, especially if occurring in strategic locations, such as the inferior frontal and cingulate gyri (van Veluw et al., 2015; De Reuck et al., 2014, 2016). Although CMIs have also been described in the cerebellum on post-mortem 7 T MRI studies, the somewhat larger cortical infarct cavities (< 1.5 cm) are more frequently observed in that region (Fig. 6) (De Reuck et al., 2015; De Cocker et al., 2014; 2013) As originally found on post-mortem 7 T MRI, those cerebellar cortical infarct cavities demonstrate a characteristic sparing of juxtacortical white matter (Fig. 6), a finding which has recently allowed translation to lower field-strength MRI in vivo (De Cocker et al., 2014; 2015). Like CMIs, cerebellar cortical infarct cavities are associated with atherosclerosis and believed to be of embolic origin (De Cocker et al., 2016; 2015).

2.2.3. Microbleeds

Detection of microbleeds may be of potential clinical relevance for a variety of pathologies, including brain trauma, hypertensive microangiopathy, cerebral amyloid angiopathy (CAA) and Alzheimer's dementia (AD) (Wardlaw et al., 2013a, b Akoudad et al., 2016; Knudsen et al., 2001; Pontes-Neto et al., 2012; Brundel et al., 2014; Bian et al., 2014). A recent post-mortem study has shown a strong association between cerebral microbleeds and CMIs in CAA, suggesting a shared underlying pathophysiologic mechanism (van Veluw et al., 2016). Susceptibility effects and the sensitivity of T2* and SWI for detecting microbleeds increase with field strength, and 3D dual-echo T2*-weighted imaging at 7 T has been found to result in better and more reliable detection of microbleeds compared with 3D T2*-weighted imaging at 1.5 T in vivo (Conijn et al.). Interestingly, a recent combined in-vivo/post-mortem MRI correlation study has shown that microbleeds on in vivo MRI are specific for microhemorrhages in CAA, but that increasing the resolution of magnetic resonance images with ultra-high resolution post mortem 7 T MRI (< 100μm isotropic voxels) results in the detection of more 'non-hemorrhagic' pathology (van Veluw et al., 2016). In addition, diagnostic confidence of rating microbleeds in vivo has not been found significantly higher at 7 T compared to 3 T for the diagnosis and exclusion of microbleeds and vascular malformations (Springer et al., 2016) .Visual rating of microbleeds is more challenging at 7 T than at lower field strengths due to the increased susceptibility effects of adjacent structures, such as veins (de Bresser et al.; Harteveld et al., 2016) Because manual detection of microbleeds may be time consuming with observer variability, automated detection systems of microbleeds have been developed (Kuijf et al., 2012, 2013; van den Heuvel et al., 2016).

2.3. Aneurysms, arteriovenous malformations and cavernomas

2.3.1. Cerebral aneurysms

7 T MRI has also been proven beneficial for the depiction of cerebral aneurysms, with overall image quality equaling the gold standard DSA (Wrede et al., 2016). 7 T has already proven its superiority over 1.5 T in the analysis of aneurysm neck and dome, as well as in the evaluation of aneurysm location at the parent vessel (Wrede et al., 2014). Using 7 T TOF MRA, microaneurysms with diameters under 1 mm are now being described, e.g. ventricular microaneurysms in patients with moyamoya disease (Matsushige et al., 2016). 7 T MPRAGE has been found superior to 7 T TOF MRA for the assessment of aneurysm features, with less artifacts and simultaneous high quality assessment of the brain with full coverage (Wrede et al., 2014). Interestingly, high-resolution vessel wall imaging has shown a strong association between ruptured aneurysms and circumferential aneurysm wall enhancement in subarachnoid hemorrhage (SAH), which may identify the site of rupture in patients with multiple intracranial aneurysms (Matouk et al., 2013, 2016 Edjlali et al., 2014; Nagahata

et al., 2014) In addition, circumferential wall enhancement has been more frequently observed in unruptured but unstable (growing and symptomatic) aneurysms (Edjlali et al., 2014; Matouk et al., 2016). Although a minority of incidentally discovered aneurysms also show wall enhancement, it still needs to be established if these are at an increased risk of rupture (Matouk et al., 2016). Apart from aneurysm vessel wall enhancement, regional differences in wall thickness of unruptured aneurysms have been demonstrated on 7 T MRI, and thinner regions have been associated with regions of higher wall shear stress determined with phase-contrast MRI (Kleinloog et al., (2014; Blankena et al., 2016). Future studies still need to address if variations in wall thickness are associated with risk of aneurysm rupture.

2.3.2. Arteriovenous malformations and cavernomas

Although DSA is still considered the gold standard for assessment of brain arteriovenous malformations (AVMs), arterial TOF MRA has become a non-invasive alternative for detection and follow-up of AVMs (Wrede et al., 2016; Matouk et al., 2016). In a recent comparative study with 1.5 T arterial TOF MRA and DSA, non-contrast-enhanced 7 T MPRAGE as well as 7 T arterial TOF MRA have been found superior to 1.5 T arterial TOF MRA in the delineation of the nidus, feeder(s), draining vein(s), and in the relationship between AVMs and adjacent vessels (non-feeding vessels relevant for surgical treatment) (Wrede et al., 2016). Compared to non-enhanced arterial TOF MRA, MPRAGE offers a very high-quality of adjacent brain structures, but is less performant in the visualization of draining veins, probably due to saturation effects of slow flowing arterialized venous blood (Wrede et al., 2016).Although overall image quality at 7 T equals DSA, all described MRA techniques at 7 T still miss dynamic information about the blood flow patterns within the AVM (Wrede et al., 2016). This may be overcome with phase contrast 4D flow imaging, which is a currently rapidly developing field and also possible at 7 T with higher SNR than at 3 T (Markl et al., 2016). Future studies will still need to assess the diagnostic potential for treatment follow-up of brain AVMs as hemorrhagic changes or artefacts due to embolic agents or clips could be misinterpreted as residual flow (Wrede et al., 2016). Also, the role of high-resolution vessel-wall MRI for brain AVMs still needs to be established.

Finally, 7 T MRI significantly improves the visualization of cavernomas and associated developmental venous anomalies (DVA) due to a higher spatial resolution and susceptibility sensitivity (Schlamann et al., 2010; Dammann et al., 2010; 2013).

3. Future directions

Different experimental and functional techniques are currently being developed and tested to assess cerebrovascular function with 7 T MRI on a microvascular level (Harteveld et al., 2016). Amongst others, these include 3D phase contrast (PC)-MRA and blood oxygenation level dependent (BOLD) functional MRI (fMRI). 7 T PC-MRA is a promising technique to visualize and measure blood flow and pulsatility, for example of the CoW and lenticulostriate arteries (van Ooij et al., 2013; Kang et al., 2016). Functional assessment with 3D PC-MRI may better discriminate between healthy and diseased arteries/arterioles compared to anatomical imaging alone, and may as such be applied to assess the relationship between white matter hyperintensities and lacunes on the one hand and blood flow in the perforating arteries on the other hand (Kang et al., 2016; Bouvy et al., 2015). BOLD fMRI, which is typically used for task-related and resting state fMRI experiments, may be adapted to measure cerebral perfusion and cerebrovascular reactivity (CVR) before and after a certain vascular challenge, such as the inhalation of carbon dioxide, breath-holding or medication administration (acetazolamide) (Harteveld et al., 2016). These stimuli all result in an increased blood flow to the brain and a decreased BOLD signal, and it is generally assumed that brain regions with a decreased signal change upon a certain challenge have a lower cerebrovascular reserve and are at an increased risk of future ischemia (Harteveld et al., 2016). At 7 T, BOLD fMRI may detect differences in cerebrovascular reactivity at a millimeter scale, and may be applied to study the association of CVR with lacunes, white matter hyperintensities and microbleeds (Conijn et al., 2012; Siero et al., 2014; Bhogal et al., 2014, 2015).

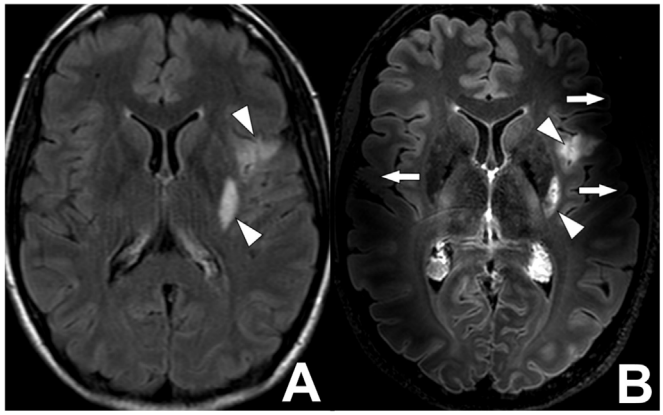

Fig. 7. B1-inhomogeneity artifacts on a 7 T MR FLAIR images of a 42-year-old female with a recent left-sided ischemic stroke. (A) A transverse 3 T FLAIR image, repetition time 10000ms, echo time 120ms, inversion time 2800 ms, acquired voxel size 0.75×1.27×4.00 mm^3, reconstructed voxel size 0.4×0.4×4.0 mm^3, field-of-view 230x182×129 mm^3, scan duration 2:00 min. No B0- or B1-inhomogeneity artifacts are seen on the image. Some patient motion is present in the image. Two hyperintense lesions are present; along the posterior margin of the left putamen and in the left insular region (white arrowheads). (B) A transverse 7 T FLAIR image, repetition time 8000ms, echo time 300 ms, inversion time 2200 ms, acquired voxel size 0.8×0.8×0.8 mm^3, reconstructed voxel size 0.5×0.5×0.5 mm^3, field-of-view 250x250×190 mm^3, scan time 10:48 min. The image is affected by B1-imhomogeniteity artefacts, best seen in both temporal lobes (white arrows). The two hyperintense lesions are seen in much more detail compared to the 3 T MR image in (A) (white arrowheads).

Despite all technical advancements, 7 T still faces some practical challenges. First, technical improvements are needed to counter the increased magnetic field (B_0) and radiofrequency field (B_1) inhomogeneities (Fig. 7). These inhomogeneities cause signal loss and a variable flip angle, most prominently in the temporal (Fig. 7) and cerebellar regions, which not only hinders the evaluation of these regions in individual subjects, but also hampers group analyses of 7 T datasets. The use of dielectric pads may partly overcome this problem. Upgraded head and neck coil technology with larger coverage and more homogenous magnetic fields are required for arterial spin labeling (ASL) perfusion imaging, which at present is still preferentially performed at 3 T (Harteveld et al., 2016). Whole brain diffusion MRI also is still challenging at 7 T due to magnetic field inhomogeneities, shorter relaxation times, and increased power deposition (specific absorption rate (SAR)), although progress is currently being made to acquire high-quality and reproducible DWI and diffusion tensor imaging (DTI) datasets (Madai et al., 2012; Vu et al., 2015; Andersson and Sotiropoulos 2016; Sotiropoulos et al., 2016). Finally, promising results on implant safety – which has long been a major drawback for clinical application – have shown no increased risk of radiofrequency heating of metallic implants (Kraff et al., 2013). These safety results and the growing evidence of an additional clinical value of 7 T MRI will pave the way towards certification for (regular) clinical applications in the near future (Madai et al., 2012).

4. Conclusion

We described the added value and emerging applications of 7 T MRI in the clinical evaluation of cerebrovascular disorders. 7 T MRI has been proven superior to lower field-strength MRI for the evaluation of the intracranial vessel lumen and vessel walls, and allows to study the brain parenchyma for microvascular pathology on a submillimeter

scale.

Acknowledgements

JH has received research support from European Research Council (ERC) grant number: ERC-2014-StG – 637024_HEARTOFSTROKE. JZ has received research support from European Research Council (ERC) grant number: ERC-2013-StG – 337333 SmallVesselMRI.

References

Akoudad, S., Wolters, F.J., Viswanathan, A., et al., 2016. Association of cerebral microbleeds with cognitive decline and dementia. JAMA Neurol.. http://dx.doi.org/10.1001/jamaneurol.2016.1017.

Andersson, J.L.R., Sotiropoulos, S.N., 2016. An integrated approach to correction for off-resonance effects and subject movement in diffusion MR imaging. Neuroimage 125, 1063–1078. http://dx.doi.org/10.1016/j.neuroimage.2015.10.019.

Aoki, S., Shirouzu, I., Sasaki, Y., et al., 1995. Enhancement of the intracranial arterial wall at MR imaging: relationship to cerebral atherosclerosis. Radiology 194, 477–481. http://dx.doi.org/10.1148/radiology.194.2.7824729.

Arai, D., Satow, T., Komuro, T., et al., 2016. Evaluation of the arterial wall in vertebrobasilar artery dissection using high-resolution magnetic resonance vessel wall imaging. J. Stroke Cerebrovasc. Dis.. http://dx.doi.org/10.1016/j.jstrokecerebrovasdis.2016.01.047.

Bernick, C., Kuller, L., Dulberg, C., et al., 2001. Silent MRI infarcts and the risk of future stroke: the cardiovascular health study. Neurology 57, 1222–1229.

Bhogal, A.A., Siero, J.C.W., Fisher, J.A., et al., 2014. Investigating the non-linearity of the BOLD cerebrovascular reactivity response to targeted hypo/hypercapnia at 7T. Neuroimage 98, 296–305. http://dx.doi.org/10.1016/j.neuroimage.2014.05.006.

Bhogal, A.A., Philippens, M.E.P., Siero, J.C.W., et al., 2015. Examining the regional and cerebral depth-dependent BOLD cerebrovascular reactivity response at 7T. Neuroimage 114, 239–248. http://dx.doi.org/10.1016/j.neuroimage.2015.04.014.

Bian, W., Hess, C.P., Chang, S.M., et al., 2014. Susceptibility-weighted MR imaging of radiation therapy-induced cerebral microbleeds in patients with glioma: a comparison between 3T and 7T. Neuroradiology 56, 91–96. http://dx.doi.org/10.1007/s00234-013-1297-8.

Blankena, R., Kleinloog, R., Verweij, B.H., et al., 2016. Thinner regions of intracranial aneurysm wall correlate with regions of higher wall shear stress: a 7T Mri study. AJNR Am. J Neuroradiol.. http://dx.doi.org/10.3174/ajnr.A4734.

Bouvy, W.H., Geurts, L.J., Kuijf, H.J., et al., 2015. Assessment of blood flow velocity and pulsatility in cerebral perforating arteries with 7-T quantitative flow MRI. NMR Biomed.. http://dx.doi.org/10.1002/nbm.3306.

Brundel, M., Reijmer, Y.D., van Veluw, S.J., et al., 2014. Cerebral microvascular lesions on high-resolution 7-Tesla MRI in patients with type 2 diabetes. Diabetes 63, 3523–3529. http://dx.doi.org/10.2337/db14-0122.

Conijn, M.M.A., Hoogduin, J.M., van der Graaf, Y., et al., 2012. Microbleeds, lacunar infarcts, white matter lesions and cerebrovascular reactivity — A 7T study. Neuroimage 59, 950–956. http://dx.doi.org/10.1016/j.neuroimage.2011.08.059.

Conijn, M.M., Geerlings, M.I., Biessels, G.-J., et al. Cerebral microbleeds on MR imaging: comparison between 1.5 and 7T. AJNR Am J Neuroradiol 32:1043–1049. http://dx.doi.org/10.3174/ajnr.A2450

Dammann, P., Barth, M., Zhu, Y., et al., 2010. Susceptibility weighted magnetic resonance imaging of cerebral cavernous malformations: prospects, drawbacks, and first experience at ultra-high field strength (7-Tesla) magnetic resonance imaging. Neurosurg. Focus 29, E5. http://dx.doi.org/10.3171/2010.6.FOCUS10130.

Dammann, P., Wrede, K.H., Maderwald, S., et al., 2013. The venous angioarchitecture of sporadic cerebral cavernous malformations: a susceptibility weighted imaging study at 7 T MRI. J. Neurol. Neurosurg. Psychiatry 84, 194–200. http://dx.doi.org/10.1136/jnnp-2012-302599.

de Bresser J, Brundel M, Conijn MM, et al. Visual cerebral microbleed detection on 7T MR imaging: reliability and effects of image processing. AJNR Am J Neuroradiol 34:E61–E64. doi: 10.3174/ajnr.A2960

De Cocker, L.J., van Veluw, S.J., Fowkes, M., et al., 2013. Very small cerebellar infarcts: integration of recent insights into a functional topographic classification. Cerebrovasc. Dis. 36, 81–87. http://dx.doi.org/10.1159/000353668.

De Cocker, L.J., van Veluw, S.J., Biessels, G.J., et al., 2014. Ischaemic cavities in the cerebellum: an ex vivo 7Tesla Mri study with pathologic correlation. Cerebrovasc. Dis. 38, 17–23, (doi: 365411).

De Cocker, L.J., Geerlings, M.I., Hartkamp, N.S., et al., 2015. Cerebellar infarct patterns: the SMART-Medea study. NeuroImage Clin. 8, 314–321. http://dx.doi.org/10.1016/j.nicl.2015.02.001.

De Cocker, L.J., Kloppenborg, R.P., van der Graaf, Y., et al., 2015. Cerebellar cortical infarct cavities: correlation with risk factors and MRI markers of cerebrovascular disease. Stroke 46, 3154–3160.

De Cocker, L.J., Compter, A., Kappelle, L.J., et al., 2016. Cerebellar cortical infarct cavities and vertebral artery disease. Neuroradiology 58, 853–857.

De Reuck, J., Deramecourt, V., Auger, F., et al., 2014. Post-mortem 7.0-tesla magnetic resonance study of cortical microinfarcts in neurodegenerative diseases and vascular dementia with neuropathological correlates. J. Neurol. Sci. 346, 85–89. http://dx.doi.org/10.1016/j.jns.2014.07.061.

De Reuck, J.L., Deramecourt, V., Auger, F., et al., 2015. The significance of cortical cerebellar microbleeds and microinfarcts in neurodegenerative and cerebrovascular diseases. A post-mortem 7.0-tesla magnetic resonance study with neuropathological correlates. Cerebrovasc. Dis. 39, 138–143. http://dx.doi.org/10.1159/000371488.

De Reuck, J.L., Auger, F., Durieux, N., et al., 2016. The topography of cortical microinfarcts in neurodegenerative diseases and in vascular dementia: a postmortem 7.0-tesla magnetic resonance imaging study. Eur. Neurol. 76, 57–61. http://dx.doi.org/10.1159/000447297.

Del Bene, A., Makin, S.D., Doubal, F.N., et al., 2013. Variations in risk factors for recent small subcortical infarcts with infarct size, shape and location. Stroke 44, 3000–3006.

Dengler NF, Madai VI, Wuerfel J, et al. (2016) Moyamoya Vessel Pathology Imaged by Ultra-High-Field Magnetic Resonance Imaging at 7.0 T. J Stroke Cerebrovasc Dis

Dieleman, N., van der Kolk, A.G., Zwanenburg, J.J., et al., 2014. Imaging intracranial vessel wall pathology with magnetic resonance imaging: current prospects and future directions. Circulation 130, 192–201. http://dx.doi.org/10.1161/CIRCULATIONAHA.113.006919.

Dieleman, N., van der Kolk, A.G., van Veluw, S.J., et al., 2014. Patterns of intracranial vessel wall changes in relation to ischemic infarcts. Neurology 83, 1316–1320. http://dx.doi.org/10.1212/WNL.0000000000000868.

Dieleman, N., van der Kolk, A.G., Zwanenburg, J.J., et al., 2016. Relations between location and type of intracranial atherosclerosis and parenchymal damage. J. Cereb. Blood Flow. Metab. 36, 1271–1280. http://dx.doi.org/10.1177/0271678X15616401.

Dieleman, N., Yang, W., Abrigo, J.M., et al., 2016. Magnetic resonance imaging of plaque morphology, burden, and distribution in patients with symptomatic middle cerebral artery stenosis. Stroke 47, 1797–1802. http://dx.doi.org/10.1161/STROKEAHA.116.013007.

Edjlali, M., Gentric, J.-C., Régent-Rodriguez, C., et al., 2014. Does aneurysmal wall enhancement on vessel wall MRI help to distinguish stable from unstable intracranial aneurysms? Stroke 45, 3704–3706. http://dx.doi.org/10.1161/STROKEAHA.114.006626.

Fanning, J.P., Wesley, A.J., Wong, A.A., et al., 2014. Emerging spectra of silent brain infarction. Stroke 45, 3461–3471. http://dx.doi.org/10.1161/STROKEAHA.114.005919.

Fracasso, A., van Veluw, S.J., Visser, F., et al., 2016. Lines of Baillarger in vivo and ex vivo: myelin contrast across lamina at 7T MRI and histology. Neuroimage 133, 163–175. http://dx.doi.org/10.1016/j.neuroimage.2016.02.072.

Ge, Y., Zohrabian, V.M., Grossman, R.I., 2008. Seven-Tesla magnetic resonance imaging: new vision of microvascular abnormalities in multiple sclerosis. Arch. Neurol. 65, 812–816. http://dx.doi.org/10.1001/archneur.65.6.812.

Gizewski, E.R., Mönninghoff, C., Forsting, M., 2015. Perspectives of ultra-high-field mri in neuroradiology. Clin. Neuroradiol. 25 (Suppl 2), 267–273. http://dx.doi.org/10.1007/s00062-015-0437-4.

Harteveld, A.A., De Cocker, L.J., Dieleman, N., et al., 2015. High-resolution postcontrast time-of-flight MR angiography of intracranial perforators at 7.0 T. PLoS One 10, e0121051. http://dx.doi.org/10.1371/journal.pone.0121051.

Harteveld, A.A., Denswil, N.P., Siero, J.C., et al., 2016. Quantitative intracranial atherosclerotic plaque characterization at 7t mri: an ex vivo study with histologic validation. AJNR Am. J. Neuroradiol. 37, 802–810. http://dx.doi.org/10.3174/ajnr.A4628.

Harteveld, A.A., van der Kolk, A.G., Zwanenburg, J.J., et al., 2016. 7-T MRI in Cerebrovascular diseases: challenges to overcome and initial results. Top. Magn. Reson. Imaging 25, 89–100. http://dx.doi.org/10.1097/RMR.0000000000000080.

Harteveld, A.A., van der Kolk, A.G., van der Worp, H.B., et al., 2016. High-resolution intracranial vessel wall MRI in an elderly asymptomatic population: comparison of 3T and 7T. Eur. Radiol.. http://dx.doi.org/10.1007/s00330-016-4483-3.

Hartkamp, N.S., Hendrikse, J., De Cocker, L.J., et al., 2016. Misinterpretation of ischaemic infarct location in relationship to the cerebrovascular territories. J. Neurol. Neurosurg. Psychiatry jnnp–2015–312906.. http://dx.doi.org/10.1136/jnnp-2015-312906.

van den Heuvel, T.L.A., van der Eerden, A.W., et al., 2016. Automated detection of cerebral microbleeds in patients with Traumatic Brain Injury. NeuroImage Clin.. http://dx.doi.org/10.1016/j.nicl.2016.07.002.

Jiang, Y., Zhu, C., Peng, W., et al., 2016. Ex-vivo imaging and plaque type classification of intracranial atherosclerotic plaque using high resolution MRI. Atherosclerosis 249, 10–16. http://dx.doi.org/10.1016/j.atherosclerosis.2016.03.033.

Kang, C.-K., Park, C.-A., Park, C.-W., et al., 2010. Lenticulostriate arteries in chronic stroke patients visualised by 7 T magnetic resonance angiography. Int. J. Stroke 5, 374–380. http://dx.doi.org/10.1111/j.1747-4949.2010.00464.x.

Kang, C.-K., Park, C.-A., Lee, D.S., et al., 2016. Velocity measurement of microvessels using phase-contrast magnetic resonance angiography at 7 T MRI. Magn. Reson. Med. 75, 1640–1646. http://dx.doi.org/10.1002/mrm.25600.

Kleinloog, R., Korkmaz, E., Zwanenburg, J.J.M., et al., 2014. Visualization of the aneurysm wall: a 7.0-tesla magnetic resonance imaging study. Neurosurg. 75:614–22; Discuss., 622. http://dx.doi.org/10.1227/NEU.0000000000000559.

Knudsen, K.A., Rosand, J., Karluk, D., et al., 2001. Clinical diagnosis of cerebral amyloid angiopathy: validation of the Boston criteria. Neurology 56, 537–539.

van der Kolk, A.G., Zwanenburg, J.J., Brundel, M., et al., 2011. Intracranial vessel wall imaging at 7.0-T MRI. Stroke 42, 2478–2484. http://dx.doi.org/10.1161/STROKEAHA.111.620443.

van der Kolk, A.G., Hendrikse, J., Brundel, M., et al., 2013. Multi-sequence whole-brain intracranial vessel wall imaging at 7.0 T. Eur. Radiol. 23, 2996–3004. http://dx.doi.org/10.1007/s00330-013-2905-z.

van der Kolk, A.G., Zwanenburg, J.J., Denswil, N.P., et al., 2015. Imaging the intracranial atherosclerotic vessel wall using 7T MRI: initial comparison with histopathology. AJNR Am. J. Neuroradiol. 36, 694–701. http://dx.doi.org/10.3174/ajnr.A4178.

Kraff, O., Wrede, K.H., Schoemberg, T., et al., 2013. MR safety assessment of potential

RF heating from cranial fixation plates at 7 T. Med. Phys. 40, 042302. http://dx.doi.org/10.1118/1.4795347.
Kuijf, H.J., de Bresser, J., Geerlings, M.I., et al., 2012. Efficient detection of cerebral microbleeds on 7.0T MR images using the radial symmetry transform. Neuroimage 59, 2266–2273. http://dx.doi.org/10.1016/j.neuroimage.2011.09.061.
Kuijf, H.J., Brundel, M., de Bresser, J., et al., 2013. Semi-automated detection of cerebral microbleeds on 3.0 T MR images. PLoS One 8, e66610. http://dx.doi.org/10.1371/journal.pone.0066610.
Küker, W., Gaertner, S., Nagele, T., et al., 2008. Vessel wall contrast enhancement: a diagnostic sign of cerebral vasculitis. Cerebrovasc. Dis. 26, 23–29. http://dx.doi.org/10.1159/000135649.
Liebeskind, D.S., Cotsonis, G.A., Saver, J.L., et al., 2011. Collateral circulation in symptomatic intracranial atherosclerosis. J. Cereb. Blood Flow. Metab. 31, 1293–1301. http://dx.doi.org/10.1038/jcbfm.2010.224.
Longstreth, W.T., Bernick, C., Manolio, T.A., et al., 1998. Lacunar infarcts defined by magnetic resonance imaging of 3660 elderly people: the Cardiovascular Health Study. Arch. Neurol. 55, 1217–1225.
Madai, V.I., von Samson-Himmelstjerna, F.C., Bauer, M., et al., 2012. Ultrahigh-field mri in human ischemic stroke - a 7 T study. PLoS One.. http://dx.doi.org/10.1371/journal.pone.0037631.
Majidi, S., Sein, J., Watanabe, M., et al., 2013. Intracranial-derived atherosclerosis assessment: an in vitro comparison between virtual histology by intravascular ultrasonography, 7T MRI, and histopathologic findings. AJNR Am. J. Neuroradiol. 34, 2259–2264. http://dx.doi.org/10.3174/ajnr.A3631.
Mandell, D.M., Matouk, C.C., Farb, R.I., et al., 2012. Vessel wall mri to differentiate between reversible cerebral vasoconstriction syndrome and central nervous system vasculitis: preliminary Results. Stroke 43, 860–862. http://dx.doi.org/10.1161/STROKEAHA.111.626184.
Markl, M., Schnell, S., Wu, C., et al., 2016. Advanced flow MRI: emerging techniques and applications. Clin. Radiol. 71, 779–795. http://dx.doi.org/10.1016/j.crad.2016.01.011.
Matouk, C.C., Mandell, D.M., Günel, M., et al., 2013. Vessel wall magnetic resonance imaging identifies the site of rupture in patients with multiple intracranial aneurysms: proof of principle. Neurosurg. 72:492–6; Discuss., 496. http://dx.doi.org/10.1227/NEU.0b013e31827d1012.
Matouk, C.C., Cord, B.J., Yeung, J., et al., 2016. High-resolution vessel wall magnetic resonance imaging in intracranial aneurysms and brain arteriovenous malformations. Top. Magn. Reson Imaging 25, 49–55. http://dx.doi.org/10.1097/RMR.0000000000000084.
Matsushige, T., Kraemer, M., Schlamann, M., et al., 2016. Ventricular microaneurysms in moyamoya angiopathy visualized with 7T MR angiography. Am. J Neuroradiol.. http://dx.doi.org/10.3174/ajnr.A4786.
Moreau, F., Patel, S., Lauzon, M.L., et al., 2012. Cavitation after acute symptomatic lacunar stroke depends on time, location, and MRI sequence. Stroke 43, 1837–1842. http://dx.doi.org/10.1161/STROKEAHA.111.647859.
Mossa-Basha, M., de Havenon, A., Becker, K.J., et al., 2016. Added value of vessel wall magnetic resonance imaging in the differentiation of moyamoya vasculopathies in a non-asian cohort. Stroke 47, 1782–1788. http://dx.doi.org/10.1161/STROKEAHA.116.013320.
Nagahata, S., Nagahata, M., Obara, M., et al., 2014. Wall enhancement of the intracranial aneurysms revealed by magnetic resonance vessel wall imaging using three-dimensional turbo spin-echo sequence with motion-sensitized driven-equilibrium: a sign of ruptured aneurysm? Clin. Neuroradiol.. http://dx.doi.org/10.1007/s00062-014-0353-z.
Obusez, E.C., Hui, F., Hajj-ali, R.A., et al., 2014. High-resolution mri vessel wall imaging: spatial and temporal patterns of reversible cerebral vasoconstriction syndrome and central nervous system vasculitis. Am. J. Neuroradiol. 35, 1527–1532. http://dx.doi.org/10.3174/ajnr.A3909.
Okuchi, S., Okada, T., Ihara, M., et al., 2013. Visualization of lenticulostriate arteries by flow-sensitive black-blood MR angiography on a 1.5 T MRI system: a comparative study between subjects with and without stroke. AJNR Am. J. Neuroradiol. 34, 780–784. http://dx.doi.org/10.3174/ajnr.A3310.
Park, S.H., Zong, X., Gao, Y., et al., 2016. Segmentation of perivascular spaces in 7T MR image using auto-context model with orientation-normalized features. Neuroimage 134, 223–235. http://dx.doi.org/10.1016/j.neuroimage.2016.03.076.
Pontes-Neto, O.M., Auriel, E., Greenberg, S.M., 2012. Advances in our understanding of the pathophysiology, detection and management of cerebral amyloid angiopathy. Eur. Neurol. Rev. 7, 134–139.
Potter, G.M., Doubal, F.N., Jackson, C.A., et al., 2010. Counting cavitating lacunes underestimates the burden of lacunar infarction. Stroke 41, 267–272. http://dx.doi.org/10.1161/STROKEAHA.109.566307.
Qiao, Y., Anwar, Z., Intrapiromkul, J., et al., 2016. Patterns and implications of intracranial arterial remodeling in stroke patient. Stroke 47, 434–440. http://dx.doi.org/10.1161/STROKEAHA.115.009955.
Raman, M.R., Preboske, G.M., Przybelski, S.A., et al., 2014. Antemortem MRI findings associated with microinfarcts at autopsy. Neurology 82, 1951–1958. http://dx.doi.org/10.1212/WNL.0000000000000471.
Riba-Llena, I., Koek, M., Verhaaren, B.F., et al., 2015. Small cortical infarcts: prevalence, determinants, and cognitive correlates in the general population. Int. J. Stroke.
Rotte, A.A., de, Koning, W., Hartog, A.G. den, et al., 2014. 7.0 T mri detection of cerebral microinfarcts in patients with a symptomatic high-grade carotid artery stenosis. J. Cereb. Blood Flow. Metab. 34, 1715–1719. http://dx.doi.org/10.1038/jcbfm.2014.141.
Saini, M., Ikram, K., Hilal, S., et al., 2012. Silent stroke: not listened to rather than silent. Stroke 43, 3102–3104. http://dx.doi.org/10.1161/STROKEAHA.112.666461.
Schlamann, M., Maderwald, S., Becker, W., et al., 2010. Cerebral cavernous hemangiomas at 7 T: initial experience. Acad. Radiol. 17, 3–6. http://dx.doi.org/10.1016/j.acra.2009.10.001.
Siero, J.C.W., Hermes, D., Hoogduin, H., et al., 2014. BOLD matches neuronal activity at the mm scale: a combined 7T fMRI and ECoG study in human sensorimotor cortex. Neuroimage 101, 177–184. http://dx.doi.org/10.1016/j.neuroimage.2014.07.002.
Sotiropoulos, S.N., Hernández-Fernández, M., Vu, A.T., et al., 2016. Fusion in diffusion MRI for improved fibre orientation estimation: an application to the 3T and 7T data of the Human Connectome Project. Neuroimage 134, 396–409. http://dx.doi.org/10.1016/j.neuroimage.2016.04.014.
Springer, E., Dymerska, B., Cardoso, P.L., et al., 2016. Comparison of routine brain imaging at 3 T and 7 T. Invest Radiol. 51, 469–482. http://dx.doi.org/10.1097/RLI.0000000000000256.
Swartz, R.H., Bhuta, S.S., Farb, R.I., et al., 2009. Intracranial arterial wall imaging using high-resolution 3-tesla contrast-enhanced MRI. Neurology 72, 627–634. http://dx.doi.org/10.1212/01.wnl.0000342470.69739.b3.
Tallantyre, E.C., Brookes, M.J., Dixon, J.E., et al., 2008. Demonstrating the perivascular distribution of MS lesions in vivo with 7-Tesla MRI. Neurology 70, 2076–2078. http://dx.doi.org/10.1212/01.wnl.0000313377.49555.2e.
van Dalen, J.W., Scuric, E.E.M., van Veluw, S.J., et al., 2015. Cortical Microinfarcts Detected In Vivo on 3 T MRI: clinical and Radiological Correlates. Stroke 46, 255–257. http://dx.doi.org/10.1161/STROKEAHA.114.007568.
van Ooij, P., Zwanenburg, J.J., Visser, F., et al., 2013. Quantification and visualization of flow in the Circle of Willis: time-resolved three-dimensional phase contrast MRI at 7 T compared with 3 T. Magn. Reson. Med. 69, 868–876. http://dx.doi.org/10.1002/mrm.24317.
van Veluw, S.J., Zwanenburg, J.J., Engelen-Lee, J., et al., 2012. In vivo detection of cerebral cortical microinfarcts with high-resolution 7T MRI. J. Cereb. Blood Flow. Metab.. http://dx.doi.org/10.1038/jcbfm.2012.196.
van Veluw, S.J., Fracasso, A., Visser, F., et al., 2015. FLAIR images at 7 T MRI highlight the ependyma and the outer layers of the cerebral cortex. Neuroimage 104, 100–109. http://dx.doi.org/10.1016/j.neuroimage.2014.10.011.
van Veluw, S.J., Hilal, S., Kuijf, H.J., et al., 2015. Cortical microinfarcts on 3T MRI: clinical correlates in memory-clinic patients. Alzheimers Dement.. http://dx.doi.org/10.1016/j.jalz.2014.12.010.
van Veluw, S.J., Zwanenburg, J.J., Rozemuller, A.J., et al., 2015. The spectrum of MR detectable cortical microinfarcts: a classification study with 7-tesla postmortem MRI and histopathology. J. Cereb. Blood Flow. Metab. 35, 676–683. http://dx.doi.org/10.1038/jcbfm.2014.258.
van Veluw, S.J., Charidimou, A., van der Kouwe, A.J., et al., 2016. Microbleed and microinfarct detection in amyloid angiopathy: a high-resolution MRI-histopathology study. Brain.. http://dx.doi.org/10.1093/brain/aww229.
van Veluw, S.J., Biessels, G.J., Klijn, C.J., et al., 2016. Heterogeneous histopathology of cortical microbleeds in cerebral amyloid angiopathy. Neurology 86, 867–871. http://dx.doi.org/10.1212/WNL.0000000000002419.
Vermeer, S.E., Prins, N.D., den Heijer, T., et al., 2003. Silent brain infarcts and the risk of dementia and cognitive decline. N. Engl. J. Med. 348, 1215–1222. http://dx.doi.org/10.1056/NEJMoa022066.
Vu, A.T., Auerbach, E., Lenglet, C., et al., 2015. High resolution whole brain diffusion imaging at 7T for the human connectome project. Neuroimage 122, 318–331. http://dx.doi.org/10.1016/j.neuroimage.2015.08.004.
Wardlaw, J.M., Smith, E.E., Biessels, G.J., et al., 2013. Neuroimaging standards for research into small vessel disease and its contribution to ageing and neurodegeneration. Lancet Neurol. 12, 822–838. http://dx.doi.org/10.1016/S1474-4422(13)70124-8.
Wardlaw, J.M., Smith, C., Dichgans, M., 2013. Mechanisms of sporadic cerebral small vessel disease: insights from neuroimaging. Lancet Neurol. 12, 483–497. http://dx.doi.org/10.1016/S1474-4422(13)70060-7.
Wrede, K.H., Dammann, P., Mönninghoff, C., et al., 2014. Non-enhanced MR imaging of cerebral aneurysms: 7 T versus 1.5 T. PLoS One 9, e84562. http://dx.doi.org/10.1371/journal.pone.0084562.
Wrede, K.H., Dammann, P., Johst, S., et al., 2016. Non-enhanced mr imaging of cerebral arteriovenous malformations at 7 T. Eur. Radiol. 26, 829–839. http://dx.doi.org/10.1007/s00330-015-3875-0.
Wrede, K.H., Matsushige, T., Goericke, S.L., et al., 2016. Non-enhanced magnetic resonance imaging of unruptured intracranial aneurysms at 7 T: comparison with digital subtraction angiography. Eur. Radiol.. http://dx.doi.org/10.1007/s00330-016-4323-5.
Zheng, L., Vinters, H.V., Mack, W.J., et al., 2013. Cerebral atherosclerosis is associated with cystic infarcts and microinfarcts but not Alzheimer pathologic changes. Stroke 44, 2835–2841. http://dx.doi.org/10.1161/STROKEAHA.113.001945.
Zhu, C., Haraldsson, H., Tian, B., et al., 2016. High resolution imaging of the intracranial vessel wall at 3 and 7 T using 3D fast spin echo MRI. Magma 29, 559–570. http://dx.doi.org/10.1007/s10334-016-0531-x.
Zong, X., Park, S.H., Shen, D., Lin, W., 2016. Visualization of perivascular spaces in the human brain at 7T: sequence optimization and morphology characterization. Neuroimage 125, 895–902. http://dx.doi.org/10.1016/j.neuroimage.2015.10.078.
Zwanenburg, J.J., Hendrikse, J., Luijten, P.R., 2012. Generalized multiple-layer appearance of the cerebral cortex with 3D FLAIR 7.0-T MR imaging. Radiology 262, 995–1001. http://dx.doi.org/10.1148/radiol.11110812.